IEEE Access
Multidisciplinary | Rapid Review | Open Access Journal

Received November 13, 2021, accepted November 25, 2021, date of publication December 10, 2021,
date of current version December 23, 2021.

Digital Object Identifier 10.1109/ACCESS.2021.3134796

Hybrid Matched Filter Detection Spectrum Sensing

ANTÓNIO BRITO[1], (Student Member, IEEE), PEDRO SEBASTIÃO[1], (Member, IEEE), AND FERNANDO J. VELEZ[2], (Senior Member, IEEE)

[1]Escola de Tecnologias e Arquitetura, Instituto de Telecomunicações and Instituto Superior de Ciências do Trabalho e da Empresa, 1649-026 Lisboa, Portugal
[2]DEM, Faculdade de Engenharia, Instituto de Telecomunicações and Universidade da Beira Interior, 6201-001 Covilhã, Portugal

Corresponding author: António Brito (ajbbo@iscte-iul.pt)

This work was supported by Fundação para a Ciência e a Tecnologia/Ministério da Ciência, Tecnologia e Ensino Superior (FCT/MCTES) through National Funds under Project UIDB/50008/2020, and in part by the CONQUEST under Project CMU/ECE/0030/2017.

ABSTRACT The radio frequency spectrum is getting more congested day by day due to the growth of wireless devices, applications, and the arrival of fifth generation (5G) mobile communications. This happens because the radio spectrum is a natural resource that has a restricted existence. Access to all devices can be granted, but in a more efficient way. To resolve the issue, cognitive radio technology has come out as a way, because it is possible to sense the radio spectrum in the neighboring. Spectrum sensing has been recognized as an important technology, in cognitive radio networks, to allow secondary users (SUs) to detect spectrum holes and opportunistically access primary licensed spectrum band without harmful interference. This paper considers the Energy Detection (ED) and Matched Filter Detection (MFD) spectrum sensing techniques as the baseline for a study where the so-called Hybrid Matched Filter Detection (Hybrid MFD) was proposed. Apart from an analytical approach, Monte Carlo simulations have been performed in MATLAB. These simulations aimed at understanding how the variation of parameters like the probability of false alarm, the signal-to-noise ratio (*SNR*) and the number of samples, can affect the probability of miss-detection. Simulation results show that i) higher probability of miss-detection is achieved for the ED spectrum sensing technique when compared to the MFD and Hybrid MFD techniques; ii) More importantly, the proposed Hybrid MFD technique outperforms MFD in terms of the ability to detect the presence of a primary user in licensed spectrum, for a probability of false alarm slightly lower than 0.5, low number of samples and low signal-to-noise ratio.

INDEX TERMS Radio frequency spectrum, 5G, cognitive radio, spectrum sensing, hybrid matched filter detection.

I. INTRODUCTION

A spectrum survey performed by the U.S. Federal Communication Commission (FCC) has stated that the licensed spectrum is not utilized correctly for numerous frequencies, time, and geographical places [1]. The available radio spectrum is a natural resource that has a restricted existence and is getting congested daily due to the increase in wireless devices and applications [2]. The year 2021 will connect over 35.85 billion wireless devices, all of which are likely going to demand access to the internet [3]. Allocating frequency channels to specific users with licenses for particular wireless technologies, is the policy that has been established regarding the allocation of radio spectrum. Licensed users have rights to send or receive data from those portions of the spectrum, while other are restricted even though those portions are unoccupied [4]. The static management of the radio spectrum is no longer effective enough to grant access to all these devices [5]. Recent studies reported that the spectrum use in the US under the fixed spectrum allocations (FSA) policy ranges anywhere from 15 percent to 85 percent [6]. Measurements made by the FCC also indicate that a wide range of radio spectrum is rarely used most of the time, while other frequency bands are heavily utilized, as shown in Figure 1. The portions of spectrum assigned to primary users (PUs) but not currently being utilized are termed white spaces or spectrum holes. In Figure 2, a spectrum hole is a frequency band allocated to a primary user that is not always used at

The associate editor coordinating the review of this manuscript and approving it for publication was Cesar Vargas-Rosales.

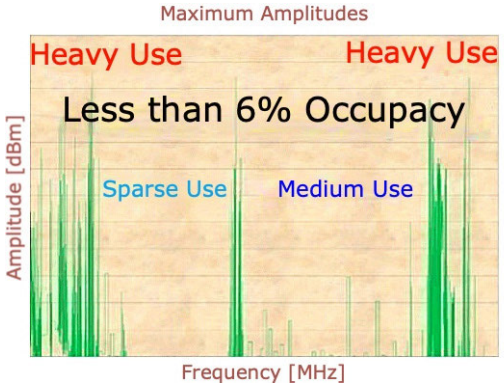

FIGURE 1. Radio spectrum occupancy, adapted from [4] with permission.

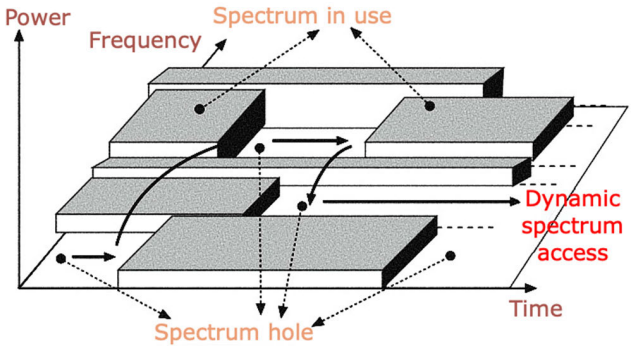

FIGURE 2. Dynamic spectrum holes, adapted from [11], with permission.

a predefined area or time. The radio spectrum is then used wastefully [6], [7].

Restricted spectrum usage, spectrum depletion and inefficient use are the main drawbacks for the underutilized wireless spectrum [8]. Consequently, urgent action is required to improve access to the radio spectrum and achieve high network capacity. A safer way to solve the spectrum shortage problem is to dynamically handle it without interfering with the PU signals by sharing unoccupied channels with unlicensed users, called secondary users (SUs). In order to resolve the problems of spectrum allocation, opportunistic spectrum access (OSA), also referred to as dynamic spectrum access (DSA), has been implemented. Unlike FSA, the DSA allows spectrum sharing between licensed and non-licensed users, in an opportunistic way, where the spectrum is split into several frequency bands assigned to one or more users, as stated in [9], [10].

In recent years, plenty of research has been done on the effective use of those spectrum bands which are either empty or are not used at full capacities. Several solutions have been suggested to advance the use of the OSA, including cognitive radio [12], [13]. CR is an adaptive and intelligent software-based technology that detects unused frequency bands and adapts the radio working parameters to communicate in these bands [14]. In the neighboring area, a cognitive radio device can fell the radio spectrum and opt to use the free channels from the licensed primary spectrum. Finding a spectrum hole through intelligent means is the primary goal of cognitive radio [15]. It enables the SUs to use the licensed radio spectrum of PU if is not being used by the PU [1] [4]. The spectrum sensing has been recognized as an important technology, in cognitive radio networks, to facilitate the detection of spectrum holes by secondary users (SUs) and opportunistically access primary licensed spectrum band without harmful interference. The wireless network will be vastly interconnected providing high coverage quality and high data rates.

Authors from [16] presented the performance analysis of energy detection scheme of spectrum sensing. This work also illustrates the impact of communication parameters such as signal-to-noise ratio (*SNR*), number of samples and noise uncertainty on the energy detector's probability of detection and false alarm. The underlying simulations were performed in MATLAB.

Authors from [17] considered the detection of the presence/ absence of signal in environments with uncertain and low *SNR*. A simple mathematical model was suggested for the uncertainty in the noise and fading processes that distinguishes which aspects contribute to the detection of *SNR* walls for different levels of signal information to be detected.

Authors from [18] comprehensively compared the performance of energy and matched filter detection spectrum sensing techniques. Simulation results plotting the operating characteristics of the receiver corroborate the theoretical results and enabled to visually compare the performance.

In [19], the matched filter method is implemented depending on various parameters. The authors discovered that the probability of detection increased when the *SNR* increases. Also, when the number of samples increases the probability of detection increases and *SNR* gets improved.

Authors from [20] propose an approach to increase the efficiency of the sensing detection by considering an estimated and dynamic sensing threshold. It simulates the matched filter method with a dynamic threshold and contrasts its performance with other existing techniques.

After analyzing the different techniques available in the literature, it is possible to know the limitations of each technique. The Energy Detection has a poor performance for low *SNR* while the Matched Filter Detection requires prior information of the primary user. In this paper, we propose a technique that, contrarily to Energy Detection, has good performance for low *SNR*, and that has better or equal performance compared to the Matched Filter Detection.

This paper describes the development, analysis, and evaluation through a set of simulations of spectrum sensing applied to CR by using MATLAB. It aims at understanding how the variation of some parameters, like the probability of false alarm, the signal-to-noise ratio, and the number of samples, can affect the probability of miss-detection. Well-known spectrum sensing techniques, like Energy Detection and Matched Filter Detection, are first considered. Then, a new Hybrid Matched Filter Detection spectrum sensing

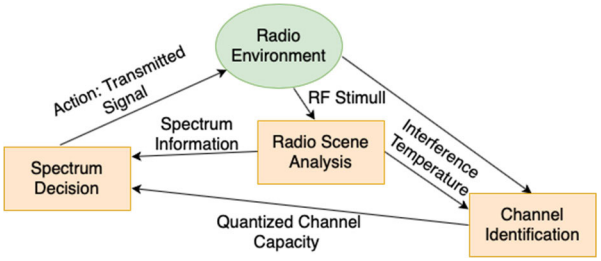

FIGURE 3. Cognitive radio cycle, adapted from [21].

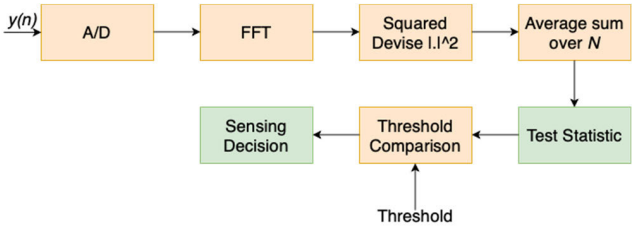

FIGURE 4. Energy detection model for spectrum sensing, adapted from [23].

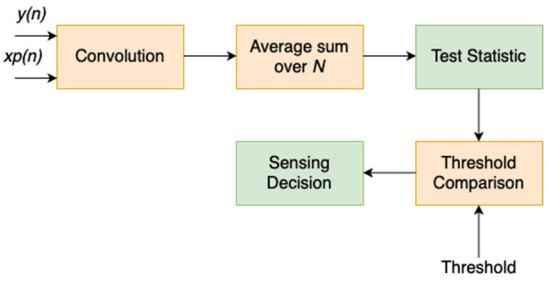

FIGURE 5. Matched filter detection for spectrum sensing, adapted from [23].

technique is explored through MATLAB simulation, and its efficiency is compared with Energy Detection and Matched Filter Detection. The proposed technique is based on the Matched Filter Detection and is hybrid because it has two different behaviors: one when the probability of false alarm is lower than 0.5 and another when it is larger or equal to 0.5.

The remaining of the paper is organized as follows. Section II discusses the background of the spectrum sensing techniques addressed in cognitive radio and the state-of-the art mathematical models for existing spectrum sensing techniques. Section III explores the mathematical model for the proposed Hybrid Matched Filter Detection. Section IV presents the simulations and results for the probability of miss-detection for the three considered techniques. Section V compares results for the probability of miss-detection between the proposed spectrum sensing technique and the previous existing ones. Conclusions are drawn in Section VI, where topics for further research are discussed as well.

II. BACKGROUND

A. COGNITIVE RADIO

The entire functioning of cognitive radio can be clarified through the cognitive radio cycle, as shown in Figure 3. In the cognitive radio cycle, a cognitive radio monitors spectrum bands collect their information and then detects spectrum spaces. The three main tasks of the cognitive radio cycle are the following ones [15]:

- Radio Scene Analysis or Spectrum Sensing, which takes care of the calculation of the interference temperature and also detects spectrum holes.
- Channel Identification or Spectrum Analysis, that is responsible for the estimation channel state information.
- Spectrum Decision has the objective of transmitting the control of power and managing the dynamic spectrum.

B. ENERGY AND MATCHED FILTER DETECTION

One of the main issues in cognitive radio is the capacity of unlicensed users (SUs) to sense the licensed users (PUs) presence in the licensed spectrum, to prevent interference and to leave the frequency band as soon as possible when the corresponding primary radio appears [22], the so-called spectrum sensing.

There are three main spectrum sensing techniques: non-cooperative sensing, cooperative sensing, and interference-based sensing. When the SU pursues its goals and does not take into detail the actions of other SUs, the non-cooperative technique is applied [23]. A cooperative technique is entirely opposite to non-cooperative because the SUs work together and collaborate with each other to take account of the goals of each user to make the final common decision [23]. Interference-based sensing enables a SU to use a licensed spectrum used by a PU, if the SU interference does not degrade the primary service quality below a tolerable limit [24]. In this paper, the focus is on non-cooperative sensing techniques, like Energy Detection [25] and Matched Filter Detection. The proposed spectrum sensing technique will also be a non-cooperative one.

1) ENERGY DETECTION

also known as radiometry or periodogram, is one of the most common and easiest techniques of spectrum sensing because of its low computational and simplicity [26]. It does not require any prior information of the PU's signal. The energy of the sensed signal is compared with the threshold to confirm whether the spectrum can be used by the secondary user [27]. The energy detector decision statistic can be determined from the squared magnitude of the Fast Fourier Transform (FFT) averaged over N samples of the SU received signal, as shown in Figure 4 [28].

2) MATCHED FILTER DETECTION

is based on a linear filter that specializes in reducing the noise component and maximizing the signal component [29]. However, this technique requires prior knowledge of the PU, which consumes more power and has high complexity [30]. The SU receives the signal and the pilot stream by assuming

that the PU transmitters sends a pilot stream simultaneously with the data. As shown in Figure 5, the decision statistic of the matched filter detector can be determined from the multiplication of the PU signal and the SU received signal averaged over N samples of the received signal by the SU [31]. The decision statistic is then compared with the threshold to confirm if it is possible to allow the secondary user to use the spectrum.

C. MATHEMATICAL MODEL FOR EXISTING SPECTRUM SENSING TECHNIQUES

Spectrum sensing algorithm efficiency depends on various parameters such as the signal-to-noise ratio, number of samples and noise uncertainty. The aim of spectrum sensing is to make a decision between two hypotheses (choose H_0 or H_1) based on the received signal [16]:

$$H_0 : y(n) = w(n), \tag{1}$$

$$H_1 : y(n) = x(n) + w(n), \tag{2}$$

where $n = 1, \ldots, N$ is the samples index of the SU received signal, $y(n)$ is the n^{th} sample of the signal received by the secondary user that might contain the primary user signal, $w(n)$ is the additive white Gaussian noise (AWGN) and $x(n)$ is the transmitted signal. H_0 denotes the primary user is absent in the band, while H_1 denotes the primary user's signal presence.

Spectrum sensing determines the presence or absence of PU based on the hypothesis problem (by choosing H_0 or H_1). By comparing the detection statistic (T) with a predetermined threshold, the decision on the occupancy of the spectrum is calculated. To evaluate the performance of the detector, several metrics, inspired by [32], were used, including the probability of false alarm, P_{fa}, and the probability of detection, P_d.

P_{fa} is the probability that H_1 is determined by the test, while it is actually H_0 given by

$$P_{fa} = \Pr(T > \lambda \mid H_0). \tag{3}$$

P_d is the probability of H_1 being correctly determined by the test, given by

$$P_d = \Pr(T > \lambda \mid H_1). \tag{4}$$

The probability of false alarm is the probability that the sensing algorithm decides the presence of PUs when they are absent. For a greater chance for the SUs to use the sensed spectrum when it is available, low probability of false alarm should be aimed. Hence, for the secondary network, the feasible throughput is greater.

The probability of detection is the time fraction in which the sensing algorithm decides correctly the presence of the PU (licensed). The performance of the system depends on the PU. If the sensing time is increased, and the limit is determined that SU cannot interfere during most of time, then the PU will make better use of its spectrum. The PUs will make best use of their priority, because the more spectrum sensing is used, the more PUs will be detected and lower the interference will be.

A good sensing algorithm is one which achieves a high probability of detection and a low probability of false alarm [15].

Determining the threshold that will be used to compare with the probabilities is another difficult task. Therefore, theoretical analysis and numerical calculations must be carried out according to practical conditions.

The dilemma of binary hypothesis testing is the core of spectrum sensing techniques. The theoretical formulation is as follows [17]:

$$y(n) = \begin{cases} w(n) & \text{under } H_0, \\ x(n) + w(n) & \text{under } H_1, \end{cases} \tag{5}$$

where $y(n)$, $w(n)$ and $x(n)$ are the received signals at CR nodes, white noise samples and transmitted signals at primary nodes, respectively.

1) ENERGY DETECTION

The detection statistic of energy detector [32] can be defined as the average energy of N observed samples, $y(n)$, given by

$$T = \frac{1}{N} \sum_{n=1}^{N} |y(n)|^2. \tag{6}$$

The average signal-to-noise ratio is defined in [17] as

$$SNR = \frac{P}{\sigma_n^2}, \tag{7}$$

where the received signal power, described in [17], is given by

$$P = \lim_{N \to \infty} \frac{1}{N} \sum_{n=1}^{N} |x(n)|^2, \tag{8}$$

and σ_n^2 is the noise variance.

The probability of false alarm [17] is given by

$$P_{fa} = Q\left(\frac{\lambda - \sigma_n^2}{\sqrt{2\sigma_n^2 / N}} \right). \tag{9}$$

The probability of detection [17] is defined as

$$P_d = Q\left(\frac{\lambda - \left(P + \sigma_n^2\right)}{\sqrt{2\left(P + \sigma_n^2\right)^2 / N}} \right). \tag{10}$$

The equations for the thresholds for the probability of false alarm are obtained by manipulating (9) and (10)

$$\lambda = Q^{-1}(P_{fa}) \cdot \sqrt{2\sigma_n^4 / N} + \sigma_n^2. \tag{11}$$

$$\lambda = Q^{-1}(P_d) \cdot \sqrt{2\left(P + \sigma_n^2\right)^2 / N} + P + \sigma_n^2. \tag{12}$$

From equations (7), (11) and (12), one can obtain the relationship between N, SNR, P_{fa} and P_d

$$P_d = Q\left(\frac{Q^{-1}\left(P_{fa}\right)\cdot\sqrt{2/N} - SNR}{\sqrt{2/N}\cdot(SNR+1)}\right). \quad (13)$$

Besides, the probability of miss-detection, described in [33], is given by

$$P_{md} = 1 - P_d. \quad (14)$$

2) MATCHED FILTER DETECTION

Matched filter is the best filter for projecting the received signal in the direction of the pilot, x_p [10]. The detection statistic [18] are given by

$$T = \frac{1}{N}\sum\nolimits_N y(n) * xp(n). \quad (15)$$

According to the Neyman-Pearson criteria [7], P_d and P_{fa} are, described in [20], expressed as

$$P_d = Q\left(\frac{\lambda - E}{\sqrt{E\sigma_n^2}}\right), \quad (16)$$

$$P_{fa} = Q\left(\frac{\lambda}{\sqrt{E\sigma_n^2}}\right), \quad (17)$$

where

$$E = \sum\nolimits_{n=1}^{N} x(n)^2. \quad (18)$$

respectively [18].

By manipulating (16) and (17), one obtains the equations for the thresholds, as follows

$$\lambda = Q^{-1}\left(P_d\right)\cdot\sqrt{E\sigma_n^2} + E. \quad (19)$$

$$\lambda = Q^{-1}\left(P_{fa}\right)\cdot\sqrt{E\sigma_n^2}. \quad (20)$$

From (19), (20) one obtains the relationship between E, P_{fa} and P_d

$$P_d = Q\left(Q^{-1}\left(P_{fa}\right) - \sqrt{\frac{E}{\sigma_n^2}}\right). \quad (21)$$

The equation for the probability of miss-detection for this technique is also (14).

III. SYSTEM MODEL FOR THE HYBRID MATCHED FILTER DETECTION TECHNIQUE

The block diagram of the proposed technique, the so-called Hybrid Matched Filter Detection (Hybrid MFD or HMFD) technique, is shown in Figure 6. This technique is based on the existing Matched Filter Detection and is combined with the double MFD. As it is hybrid it has two different behaviors, one when the probability of false alarm is lower than 0.5 and another when it is larger or equal to 0.5.

Whenever the probability of false alarm is lower than 0.5, the second part of the detector (from Figure 6), which

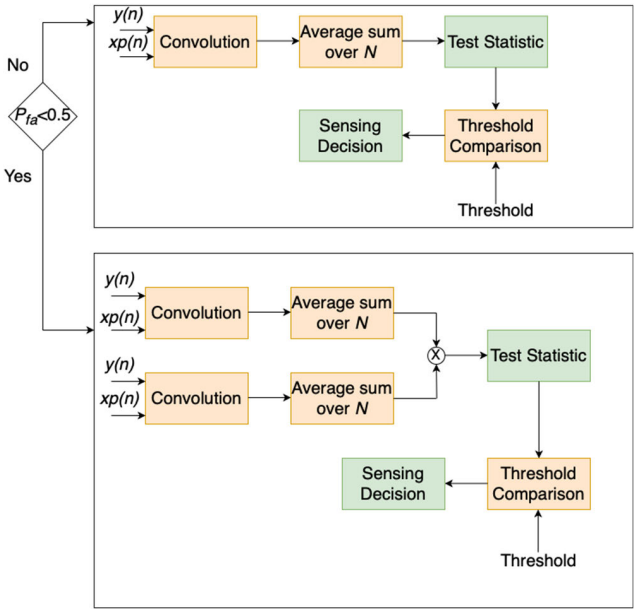

FIGURE 6. Proposed model for the hybrid matched filter detection technique.

corresponds to a double matched filter detector, is used. This double matched filter detector is a new technique and basically corresponds on the multiplications of two normal matched filter detector, where the detection statistic consists of a multiplication of two detection statistic and the threshold is the multiplication of two threshold from a normal matched filter detector. When the probability of false alarm is larger than or equal to 0.5, the first detector, i.e., a normal matched filter detector, is used.

The detection statistic of the detector corresponding to $P_{fa} < 0.5$ is given as follows:

$$T = \frac{1}{N}\sum\nolimits_N y(n) * xp(n) \cdot \frac{1}{N}\sum\nolimits_N y(n) * xp(n). \quad (22)$$

The detection statistic of the detector corresponding to $P_{fa} >= 0.5$ is given by (15). The threshold of the detector for corresponding to $P_{fa} < 0.5$, is given by

$$\lambda = \left(Q^{-1}\left(P_{fa}\right)\cdot\sqrt{E\sigma_n^2}\right)^2. \quad (23)$$

The threshold of the detector corresponding to $P_{fa} >= 0.5$ is given by (20).

Figure 7 presents curves from the results of the simulations for the matched filter detector (orange curve) and double matched filter detector (blue curve) for values of the probability of the false alarm varying from 0 to 1, using the same samples and SNR.

In Figure 7, for values of the probability of false alarm lower than 0.5, the double matched filter detector achieves better performance compared to a matched filter detector. For values of the probability of false alarm larger than or equal to 0.5, the probability of miss-detection starts to increase for the double matched filter detector, up to a point where the

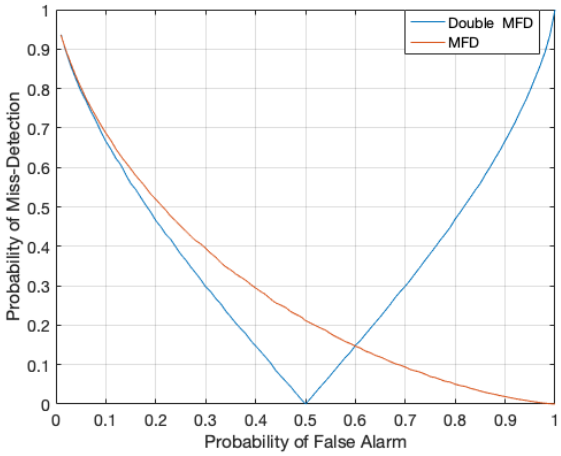

FIGURE 7. Probability of miss-detection for the simulated matched filter and double matched filter detection.

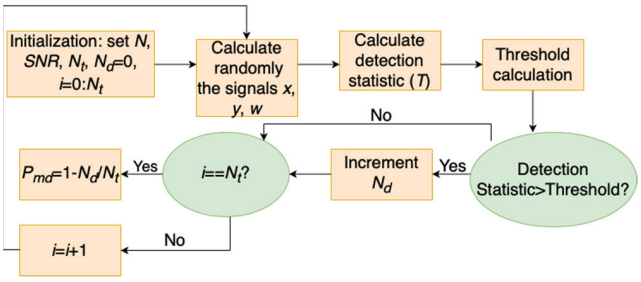

FIGURE 8. Algorithm used to calculate the probability of miss-detection.

matched filter detector has better performance compared to the double matched filter detector.

The probability of miss-detection is computed by using the algorithm described in the flowchart of Figure 8, where N_t is the number of Monte-Carlo simulations, N_d is the number of iterations used for the calculation of the probability of miss-detection, and P_{fa} is the probability of false alarm, in the range from zero to one.

The algorithm to compute the probability of miss-detection is very similar for the ED and MFD. First, we must set the number of samples (N), the signal-to-noise ratio (SNR) and the number of Monte-Carlo simulations, N_t. Then, there will be a *for* cycle that will go through the values of the probabilities of false alarm, from 0 to 1, with steps of 0.01. Inside this *for* cycle there will be another *for* cycle that will start in zero and go up to the number of Monte-Carlo simulations. A new variable, i, is going to be used to see know many simulations Monte-Carlo have been done and how many there are left. For each Monte-Carlo simulation, the additive white Gaussian noise, w, and transmitted signal, x, are randomly generated by using the *randn* function with mean equal to zero. By considering this approach, signals may have positive or negative values. The signal received by the secondary user is y, according to (5).

The detection statistic is calculated as follows:

- for the Energy Detection, equation (6) is used, and the result for the detection statistic will always be positive,
- for the Matched Filter Detection, equation (15) is used, and the result can be a positive or a negative number.

The probability of false threshold for the Energy Detection is calculated by considering (11) while equation (20) is used for the Matched Filter Detection. On the one hand, according to (11), this threshold is always positive for the Energy Detection because the value in the second portion of the equation is always larger than for the first one, and they are summed. On the other hand, the threshold for the Matched Filter Detection may be a positive or a negative number, or even also null. This occurrence is justified by the behavior of the Q^{-1} function, which varies as follows:

- it is positive for a $P_{fa} < 0.5$;
- it is negative for a $P_{fa} > 0.5$;
- it is zero for a $P_{fa} = 0.5$.

One needs to verify if the detection statistic is larger than the threshold. If the detection statistic is lower than the threshold, one checks if the variable i is equal to N_t. This condition is met when all the Monte-Carlo simulations have already been concluded for each value of the probability of false alarm. If the variable i is equal to the N_t, the probability of miss-detection is given by $1 - N_d/N_t$. Then the simulation is over for this probability of false alarm. If the variable i and N_t are not the same, the variable i will be incremented and on will perform another Monte-Carlo simulation by starting to randomly generate the signals. If the detection statistic is larger than the threshold, we will increment the variable N_d. Then, one has to verify if the variable i, is equal to N_t, like it was described before. Finally, one verifies if all Monte-Carlo simulations have been concluded for the current value of the probability of false alarm. If this is true, then one is able to calculate the probability of miss-detection for the current value of the probability of false alarm; otherwise, another simulation must be performed, until all the Monte-Carlo simulations are performed for all probabilities of false alarm, and a plot is generated.

In the case of the Double MFD, the procedure to compute the probability of miss-detection is very similar to the MFD. The only differences are that the detection statistic and the threshold are the square of their values for the MFD.

For the Double MFD, the detection statistic and threshold are calculated as follows:

- equation (22) is used for the detection statistic, and the result is always positive,
- equation (23) is used to compute the threshold, and the result is always a positive number, unless for $P_{fa} = 0.5$ because it is zero.

This occurs because the square of a Q^{-1} function is positive for all the probabilities of false alarm, but not for $P_{fa} = 0.5$ (when it is zero). As described before, the Q^{-1} function is positive for $P_{fa} < 0.5$, it is negative for $P_{fa} > 0.5$ and is zero for a $P_{fa} = 0.5$. The Q^{-1} function is given by $Q^{-1}(P_{fa}) = -Q^{-1}(1 - P_{fa})$. The square of the Q^{-1} function is given by

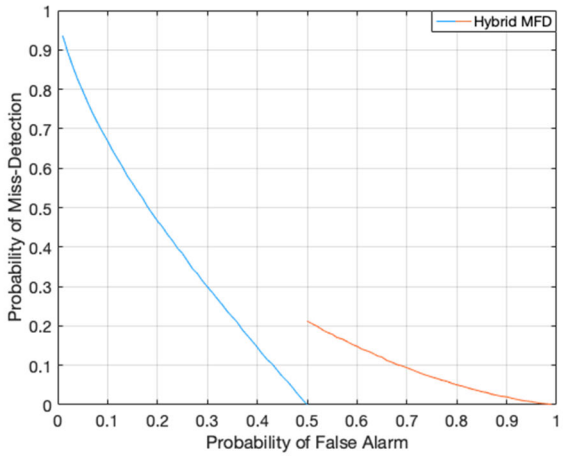

FIGURE 9. Probability of miss-detection vs probability of false alarm for the hybrid matched filter detection technique.

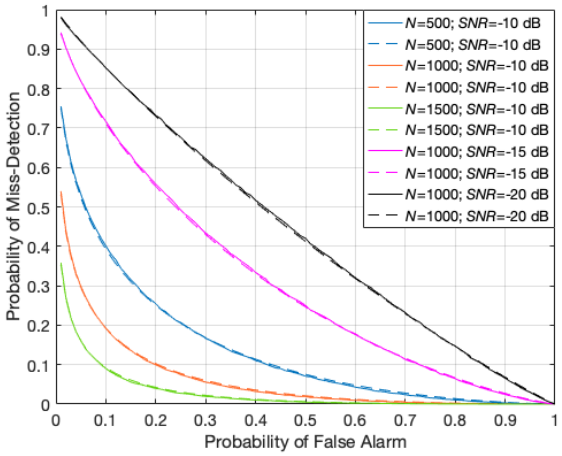

FIGURE 10. Probability of miss-detection vs probability of false alarm for the energy detection technique with the number of samples and *SNR* as parameters.

$(Q^{-1}(P_{fa}))^2 = (-Q^{-1}(1-P_{fa}))^2$. Basically, it is like having a mirror in the view chart for $P_{fa} = 0.5$. The rest of the simulation proceeds like for the previous two sensing techniques. Figure 7 presents just one example of the simulations that have been performed by changing the number of samples and the *SNR* value. The intersection point between the curves for the two techniques (MFD and Double MFD) would always change, because the signals are randomly generated.

By applying the HMFD algorithm, results have been obtained for the probability of miss-detection as a function of the probability of false alarm, as shown in Figure 9.

In the proposed model, while obtaining results for the HMFD, it was decided to consider the probability of false alarm of 0.5 to switch between different techniques (blue part of the curve for the Double MFD and orange part for the MFD), since, in the double matched filter detector, the probability of miss-detection is always zero when the probability of false alarm is 0.5, as shown in Figure 9.

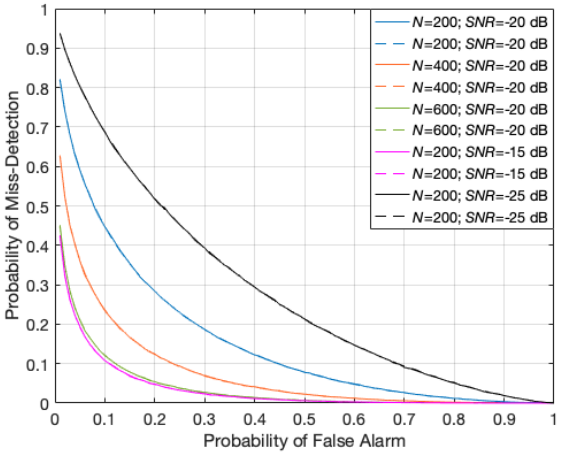

FIGURE 11. Probability of miss-detection vs probability of false alarm for the matched filter detection technique with the number of samples and *SNR* as parameters.

IV. SIMULATIONS AND RESULTS

In this section, results for the probability of miss-detection arising from Monte-Carlo simulations results are obtained to verify the theoretical expressions derived above. To evaluate the influence of the number of samples, probability of false alarm and *SNR* in the probability of miss-detection, one uses MATLAB to simulate and analyze different techniques whilst varying the parameters.

Because of the complexity of the expression of the HMFD technique, it is only possible to obtain results through a Monte-Carlo simulation approach.

The following three types of analysis are performed:

- The first option corresponds to curves where the probability of miss-detection (Y-axis) is presented as a function of the probability of false alarm (X-axis), with the number of samples and *SNR* as parameters.
- The second option corresponds to curves where the probability of miss-detection (Y-axis) is presented as a function of the number of samples (X-axis), with the probability of false alarm and *SNR* as parameters.
- The third option corresponds to curves where the probability of miss-detection (Y-axis) is presented as a function of the *SNR* (X-axis), with the probability of false alarm and number of samples as parameters.

A. FIRST OPTION

Figures 10, 11 and 12 present the results for the probability of miss-detection as a function of the probability of false alarm, P_{fa}, with the number of samples, N, and *SNR* as parameters, for the Energy Detection (ED), Matched Filter Detection (MFD) and Hybrid MFD techniques, respectively. Each figure presents theoretical (dashed lines) and simulation results (solid lines).

One considers different combinations of the values for the number of samples and *SNR*. The Energy Detection technique has been simulated by considering equations (3),

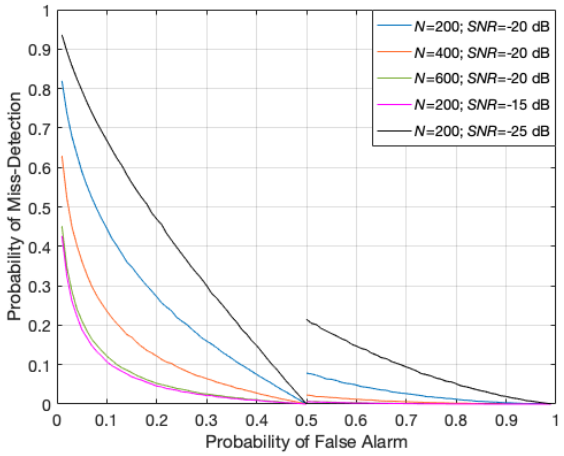

FIGURE 12. Probability of miss-detection vs probability of false alarm for the hybrid matched filter detection technique with the number of samples and *SNR* as parameters.

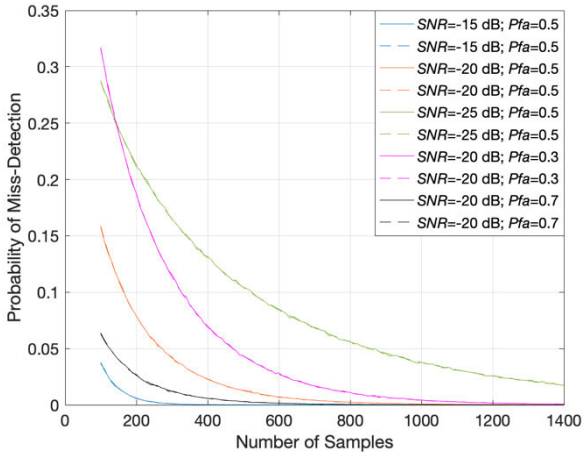

FIGURE 14. Probability of miss-detection vs number of samples for the matched filter detection technique with the probability of false alarm and *SNR* as parameters.

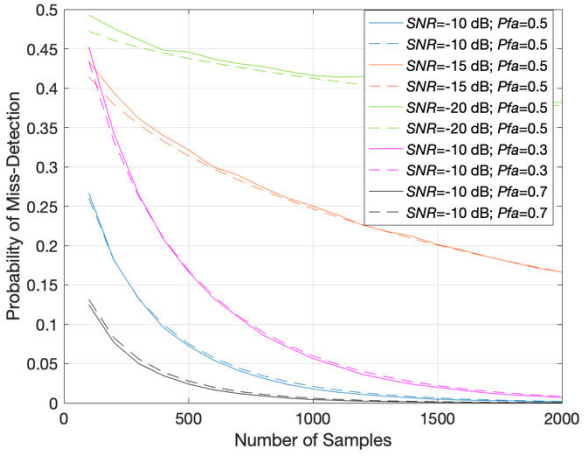

FIGURE 13. Probability of miss-detection vs number of samples for the energy detection technique, with the probability of false alarm and *SNR* as parameters.

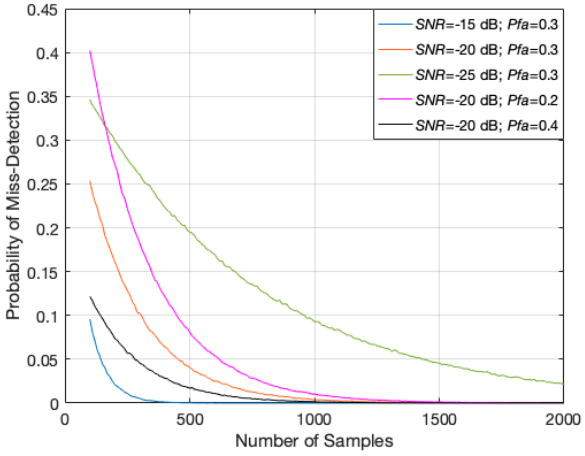

FIGURE 15. Probability of miss-detection vs number of samples for the hybrid matched filter detection technique with the probability of false alarm and *SNR* as parameters.

(4), (6) and (11) while theoretical results are achieved by using (13). On the other hand, For the MFD and HMFD techniques, simulation results are achieved by considering equations (3), (4), (15) and (20) (and additionally (22) and (23) for the HMFD only). Besides, theoretical results for the MFD spectrum sensing technique are achieved by using (21). One observes that the probability of false alarm always varies from 1 down to 0. As expected, for the HMFD technique, there is a discontinuity for $P_{fa} = 0.5$.

One may conclude that the probability of miss-detection decreases when:

- the probability of false alarm increases;
- the *SNR* increases for a given number of samples;
- the number of samples increase for a given value of *SNR*.

B. SECOND OPTION

Figures 13, 14 and 15 present the results for the probability of miss-detection as a function of the number of samples, with the *SNR* and P_{fa} as parameters, for the ED, MFD and HMFD spectrum sensing techniques, respectively. Each figure presents theoretical (dashed lines) and simulation results (solid lines). While in Figure 14 the number of samples varies from 100 up to 1400, in Figures 13 and 15 it varies from 100 up to 2000.

One may conclude that the probability of miss-detection decreases when:

- the number of samples increases;
- the *SNR* increases for a given probability of false alarm;
- the probability of false alarm increases for a given value of *SNR*.

C. THIRD OPTION

Figures 16, 17 and 18 present results for the probability of miss-detection as a function of the *SNR*, with the probability of false alarm and the number of samples as parameters, for the ED, MFD and HMFD spectrum sensing techniques,

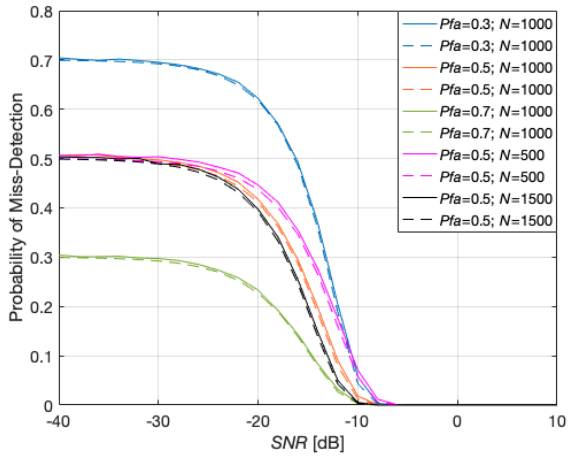

FIGURE 16. Probability of miss-detection vs *SNR* for the energy detection technique with the probability of false alarm and number of samples as parameters.

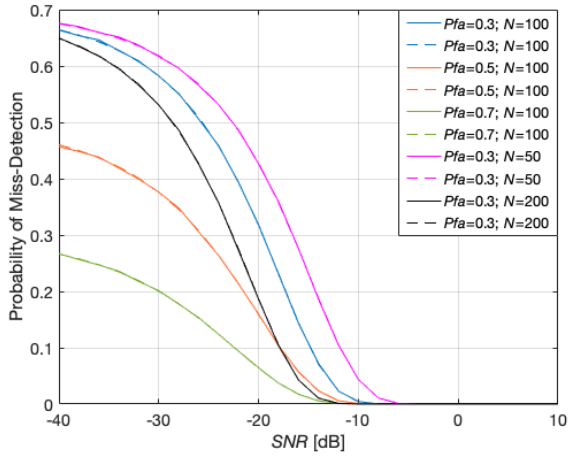

FIGURE 17. Probability of miss-detection vs *SNR* for the matched filter detection technique with the probability of false alarm and number of Samples as parameters.

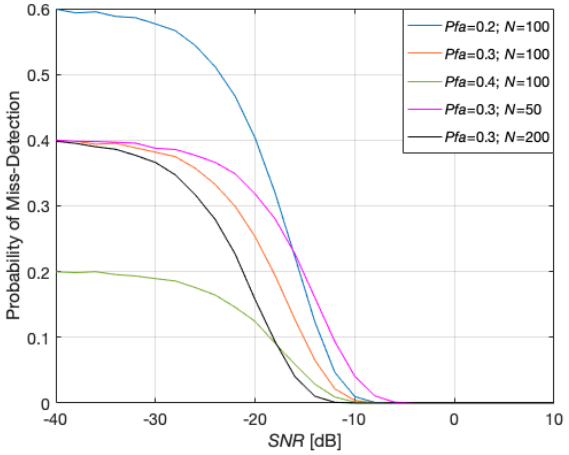

FIGURE 18. Probability of miss-detection vs *SNR* for the hybrid matched filter detection technique with the probability of false alarm and number of samples as parameters.

respectively, where the *SNR* varies from −40 dB up to 10 dB. As above, each figure presents theoretical (dashed lines) and simulation results (solid lines).

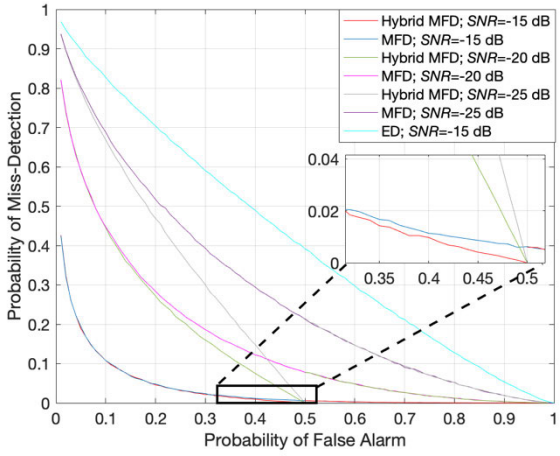

FIGURE 19. Probability of miss-detection as a function of the probability of false alarm for $N = 200$.

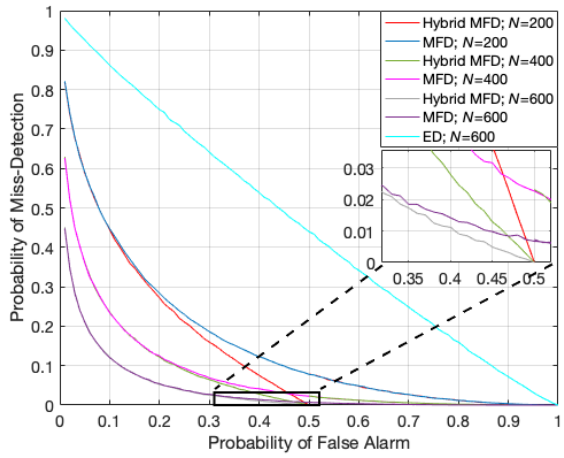

FIGURE 20. Probability of miss-detection as a function of the probability of false alarm for $SNR = -20$ dB.

One may conclude that the probability of miss-detection decreases when:

- the *SNR* increases;
- the probability of false alarm increases for a given number of samples;
- the number of samples increases for a given value of the probability of false alarm.

V. COMPARISON BETWEEN TECHNIQUES

It is worthwhile to analyze the results for the probability of miss-detection between different spectrum sensing techniques. In Figures 19 and 20 the probability of miss-detection is represented as a function of the probability of false alarm. In Figure 19, the number of samples is $N = 200$ while *SNR* takes values of −25, −20 and −15 dB (except for the ED sensing technique, where only $SNR = -15$ dB was accounted for). In Figure 20, one considers $SNR = -20$ dB, and the number of samples takes values of 200, 400 and 600 (except for the ED sensing technique, where only $N = 600$ was

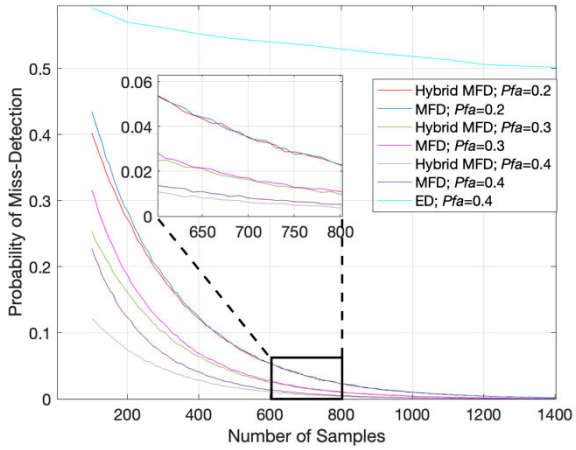

FIGURE 21. Probability of miss-detection as a function of the number of samples for $SNR = -20$ dB.

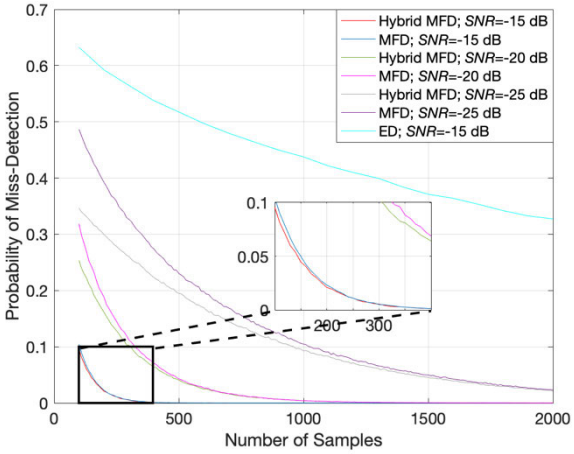

FIGURE 22. Probability of miss-detection as a function of the number of samples for $P_{fa} = 0.3$.

considered). **N.B.:** in Figures 19 and 20, although the behavior of the Hybrid MFD is similar to the one from the MFD when the probability of false alarm is equal or larger than 0.5, when the probability of false alarm increases towards 0.5, in the zoom out view charts, one can observe that the probability of miss-detection is lower for the HMFD.

Table 1 summarizes the lessons learned from the analysis of the results for the probability of miss-detection as a function of the probability of false alarm of Figures 19 and 20.

Figures 21 and 22 present results for the probability of miss-detection as a function of the number of samples while comparing different spectrum sensing techniques. While in Figure 21 the probability of false alarm is a varying parameter (except for the ED sensing technique, where only $P_{fa} = 0.4$ was considered) and $SNR = -20$ dB.

In Figure 22 *SNR* takes different values (except for the ED sensing technique, where only $SNR = -15$ dB was considered) and $P_{fa} = 0.3$. Table 2 presents the lessons learned.

TABLE 1. Comparison of the probability of miss-detection as a function of the probability of false alarm between different techniques and the underlying impact of the probability of false alarm, number of samples and *SNR*.

When	What happens
The *SNR* and the number of samples are lower	There is a clear difference between the MFD and the HMFD
The probability of false alarm is slightly lower than 0.5	The performance of the HMFD technique is higher than with MFD, since it achieves the lowest probability of miss-detection for the same number of samples and *SNR*
The *SNR* and number of samples are larger	The ED has the worst performance since it has a larger probability of miss-detection for the same P_{fa}

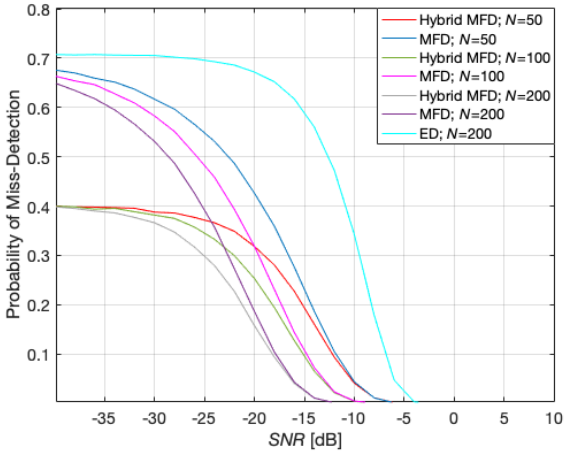

FIGURE 23. Comparison between techniques for the probability of miss-detection vs *SNR* for $P_{fa} = 0.3$.

N.B.: in Figure 21, the HMFD has lower probability of miss-detection when comparing with MFD, for $P_{fa} = 0.2$, $P_{fa} = 0.3$ and $P_{fa} = 0.4$, up to a number of samples of 300, 620 and 800, respectively, as it is possible to observe in the zoom out view charts. Beyond those values of N, the behavior of the HMFD and MFD is similar. In Figure 22, the values of the probability of miss-detection for the HMFD technique is lower than for the MFD technique for $SNR = -15$ dB, $SNR = -20$ dB and $SNR = -25$ dB, up to $N = 280$, 420, and 1700, respectively. For higher values of the number of samples, the behavior of the HMFD and MFD SS techniques is similar.

Figures 23 and 24 present results for the probability of miss-detection as a function of the *SNR* while comparing different spectrum sensing techniques. In Figure 23, one considers $P_{fa} = 0.3$ while the number of samples takes different values (except for the ED sensing technique, where only $N = 200$ was considered).

In Figure 24, one considers $N = 100$ while the probability of false alarm varies (except for the ED sensing technique, where only $P_{fa} = 0.4$ was considered). **N.B.:** in Figure 23, the Hybrid MFD (or HMFD) has a lower probability of miss-detection when comparing with the MFD, for $N = 50$, $N = 100$ and $N = 200$, until the *SNR* of -10 dB, -12 dB and

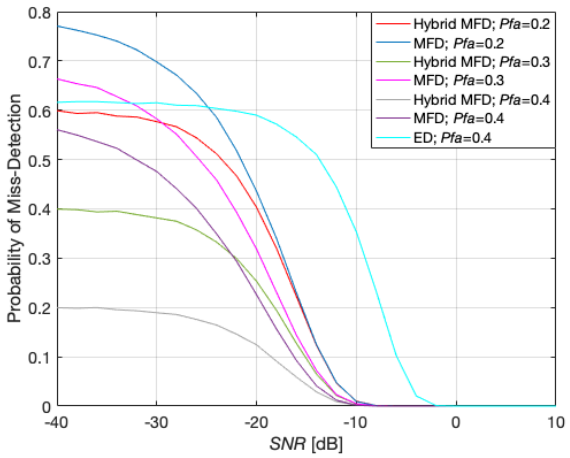

FIGURE 24. Comparison between techniques for the probability of miss-detection vs *SNR* for $N = 100$.

TABLE 2. Comparison of the probability of miss-detection as a function of N between different techniques and the underlying impact of the N, *SNR* and probability of false alarm.

When	What happens
The probability of false alarm is slightly lower than 0.5 and *SNR* takes the lowest values	There is a more evident difference between the MFD and the HMFD
The number of samples is low	The performance of the HMFD is higher than with the MFD, since it has lower probability of miss-detection for the same *SNR* and probability of false alarm
The *SNR* and P_{fa} are larger	The ED has the worst performance since it achieves a larger probability of miss-detection for the same number of samples

TABLE 3. Comparison between techniques for the probability of miss-detection as a function of the *SNR* and the impact of the *SNR*, probability of false alarm and N in the comparison.

When	What happens
The probability of false alarm is slightly lower than 0.5 and number of samples is the lowest	It is possible to have a more evident difference between the MFD and the HMFD
The *SNR* has the lowest values	The performance of HMFD is higher than with the simple MFD, since it has lower probability of miss-detection for the same number of samples and P_{fa}
The number of samples and probability of false alarm are larger	The ED has the worst performance since it achieves a larger probability of miss-detection for the same *SNR*

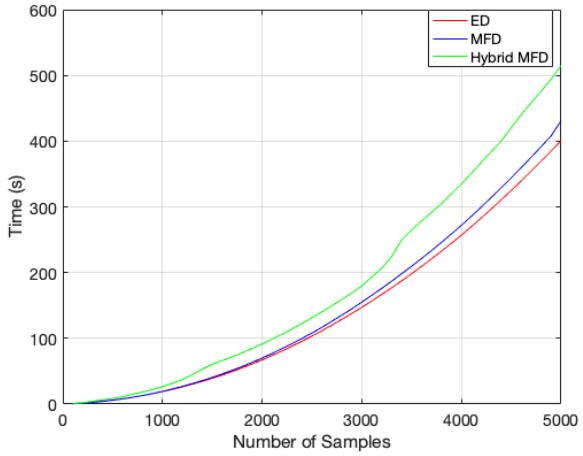

FIGURE 25. Comparison between techniques for the time vs number of samples with $P_{fa} = 0.3$ and $SNR = -25$ dB.

-16 dB, respectively. After those values of *SNR*, the behavior of the Hybrid MFD and MFD is similar.

In Figure 24, for $P_{fa} = 0.2$, $P_{fa} = 0.3$ and $P_{fa} = 0.4$, the probability of miss-detection is lower when comparing with the MFD, until the *SNR* of -14 dB, -12 dB, and -10 dB, respectively. For higher *SNR*, the HMFD and MFD behaviors are similar.

Table 3 summarizes the lessons learned from the analysis of the results for the probability of miss-detection as a function of the *SNR* of Figures 23 and 24.

As a measure of the computational complexity, Figure 25 compares results for the algorithm simulation running time (in seconds), for a given N, between different spectrum sensing techniques. In Figure 25, one considers $P_{fa} = 0.3$ and $SNR = -25$ dB. The computational complexity is $O(N^2)$ for all considered spectrum sensing techniques. In Figure 25, when N increases, the running time also increases. The higher N is, the larger the difference between the three spectrum sensing techniques is. While the ED sensing technique requires 401s to simulate 5000 samples, MFD and HMFD require 431s and 515s, respectively, s to accomplish the same task. When compared to the other existing techniques, like ED and MFD, the proposed HMFD sensing technique will certainly allow the SUs to better detect the spectrum holes under various circumstances, while opportunistically accessing primary licensed bands without harmful interference.

VI. CONCLUSION AND FUTURE WORK

In this paper, we have proposed the Hybrid Matched Filter Detection (HMFD), a new non-cooperative spectrum sensing technique, based on the existing Matched Filter Detection, that combines different behaviors when the probability of false alarm is lower than 0.5 or when it is larger or equal to 0.5.

The HMFD technique has been compared to other state-of-the-art techniques, like Energy Detection (ED) and Matched Filter Detection (MFD). First, these techniques have been analyzed separately to understand the impact in the probability of miss-detection of changing given parameters, like the signal-to-noise ratio, probability of false alarm and number of samples, N. Secondly, these techniques have been compared by considering the same parameters to try and understand which of them are more efficient. A high coincidence is achieved between the simulation and theoretical approaches.

Results show that the MFD and HMFD techniques outperform the ED technique for the same set of parameters. Besides, by comparing the MFD and the HMFD in terms of the ability to detect the presence of primary user, one conclude that the proposed technique outperforms the MFD in licensed spectrum, as follows:

- for low N and SNR (in the view chart of probability of miss-detection as a function of the probability of false alarm);
- for a probability of false alarm slightly lower than 0.5 and low SNR (in the view chart of the probability of miss-detection as a function of N);
- for a probability of false increasing towards 0.5 and low N (in the view chart of the probability of miss-detection as a function of SNR).

Finally, it is worthwhile to note that although the computational complexity is $O(N^2)$ for all considered spectrum sensing techniques, to simulate 5000 samples, the simulation running time slightly increases (from 401-431 s to 515 s) for the HMFD.

One aspect to be explored in future work may be the proposal of theorical equations for the HMFD technique since, in this work, these results have only been extracted by Monte-Carlo simulations. Another aspect to be explored can be the proposal of a new high-performance non-cooperative spectrum sensing based on Cyclostationary Detection. The study the other performance metrics can also be explored. We may, in a possible practical cognitive radio scenario, also transmit a signal using, e.g., a Raspberry Pi 3 card, and detect it by using the proposed spectrum sensing technique implemented in MATLAB, connected to, e.g., an RealTek-Software Defined Radio. The proposed application will be evaluated in terms of the detector ability to identify the presence of the signal in the shared spectrum.

ACKNOWLEDGMENT

The authors would like to thank Fatima Salahdine and Ian Akyildiz for allowing we to reuse their figures in Figure 1 and Figure 2 from this paper, respectively.

REFERENCES

[1] N. Kaabouch and W.-C. Hu, *Handbook of Research on Software-Defined and Cognitive Radio Technologies for Dynamic Spectrum Management*. Hershey, PA, USA: IGI Global, 2014.

[2] M. Subhedar and G. Birajdar, "Spectrum sensing techniques in cognitive radio networks: A survey," *Int. J. Next-Gener. Netw.*, vol. 3, no. 2, pp. 37–51, 2011.

[3] *Techjury*. Accessed: Apr. 15, 2021. [Online]. Available: https://techjury.net/blog/how-many-iot-devices-are-there/#gref

[4] F. Salahdine and H. El Ghazi, "A real time spectrum scanning technique based on compressive sensing for cognitive radio networks," in *Proc. IEEE 8th Annu. Ubiquitous Comput., Electron. Mobile Commun. Conf. (UEMCON)*, Oct. 2017, pp. 1–6.

[5] Y. Arjoune and N. Kaabouch, "A comprehensive survey on spectrum sensing in cognitive radio networks: Recent advances, new challenges, and future research directions," *Sensors*, vol. 19, no. 1, p. 126, Jan. 2019.

[6] H. Reyes, S. Subramaniam, N. Kaabouch, and W. C. Hu, "A spectrum sensing technique based on autocorrelation and Euclidean distance and its comparison with energy detection for cognitive radio networks," *Comput. Electr. Eng.*, vol. 52, pp. 319–327, May 2016.

[7] X. Lu, P. Wang, D. Niyato, and E. Hossain, "Dynamic spectrum access in cognitive radio networks with RF energy harvesting," *IEEE Wireless Commun.*, vol. 21, no. 3, pp. 102–110, Jun. 2014.

[8] D. Cabric, S. M. Mishra, and R. W. Brodersen, "Implementation issues in spectrum sensing for cognitive radios," in *Proc. Conf. Rec. 38th Asilomar Conf. Signals, Syst. Comput.*, vol. 1, Nov. 2004, pp. 772–776.

[9] N. Armi, M. Z. Yusoff, and N. M. Saad, "Decentralized cooperative user in opportunistic spectrum access system," in *Proc. 4th Int. Conf. Intell. Adv. Syst. (ICIAS)*, vol. 1, 2012, pp. 179–183.

[10] N. Armi, M. Z. Yusoff, N. M. Saad, and B. S. Iskandar, "Cooperative spectrum sensing in decentralized cognitive radio system," in *Proc. Eurocon*, Jul. 2013, pp. 113–118.

[11] I. F. Akyildiz, W.-Y. Lee, M. C. Vuran, and S. Mohanty, "A survey on spectrum management in cognitive radio networks," *IEEE Commun. Mag.*, vol. 46, no. 4, pp. 40–48, Apr. 2008.

[12] A. Ghasemi and E. S. Sousa, "Spectrum sensing in cognitive radio networks: Requirements, challenges and design trade-offs," *IEEE Commun. Mag.*, vol. 46, no. 4, pp. 32–39, Apr. 2008.

[13] Ž. Tabaković, "A survey of cognitive radio systems," *Post Electron. Commun. Agency*, vol. 13, no. 1, pp. 1–8, 2011.

[14] J. Mitola, "Cognitive radio: An integrated agent architecture for software-defined radio," Ph.D. dissertation, KHT Roy. Inst. Technol., Stockholm, Sweden, 2009.

[15] S. Haykin, "Cognitive radio: Brain-empowered wireless communications," *IEEE J. Sel. Areas Commun.*, vol. 23, no. 2, pp. 201–220, Feb. 2005.

[16] M. Joshi and S. Borde, "Comprehensive analysis of various energy detection parameters in spectrum sensing for cognitive radio systems," in *Proc. Int. Conf. Adv. Commun. Comput. Technol. (ICACACT)*, Aug. 2014, pp. 1–4.

[17] R. Tandra and A. Sahai, "SNR walls for signal detection," *IEEE J. Sel. Topics Signal Process.*, vol. 2, no. 1, pp. 4–17, Feb. 2008.

[18] D. Bhargavia and C. Murthy, "Performance comparison of energy, matched-filter and cyclostationarity-based spectrum sensing," in *Proc. IEEE 11th Int. Workshop Signal Process. Adv. Wireless Commun. (SPAWC)*, Jun. 2010, pp. 1–5.

[19] B. A. Odhavjibhai and S. Rana, "Analysis of matched filter based spectrum sesning in cognitive radio," *Int. Res. J. Eng. Technol.*, vol. 4, no. 4, pp. 578–581, Apr. 2017.

[20] F. Salahdine, H. E. Ghazi, N. Kaabouch, and W. F. Fihri, "Matched filter detection with dynamic threshold for cognitive radio networks," in *Proc. Int. Conf. Wireless Netw. Mobile Commun. (WINCOM)*, Sep. 2015, pp. 1–6.

[21] R. Kumar, "Analysis of spectrum sensing techniques in cognitive radio," *Int. J. Inf. Comput. Technol.*, vol. 4, no. 4, pp. 437–444, 2014.

[22] A. M. Jasim and H. N. Al-Anbagi, "A comprehensive study of spectrum sensing techniques in cognitive radio networks," in *Proc. Int. Conf. Current Res. Comput. Sci. Inf. Technol. (ICCIT)*, Apr. 2017, pp. 107–114.

[23] F. Salahdine, "Spectrum sensing techniques for cognitive radio networks," 2017, *arXiv:1710.02668*.

[24] A. Fanan, N. Riley, M. Mehdawi, M. Ammar, and M. Zolfaghari, "Survey: A comparison of spectrum sensing techniques in cognitive radio," in *Proc. Conf. Image Process., Comput. Ind. Eng.*, Jun. 2014, pp. 65–69.

[25] H. Urkowitz, "Energy detection of unknown deterministic signals," *Proc. IEEE*, vol. 55, no. 4, pp. 523–531, Apr. 1967.

[26] P. Pawelczak, G. J. M. Janssen, and R. V. Prasad, "Performance measures of dynamic spectrum access networks," in *Proc. IEEE Globecom*, Francisco, CA, USA, Nov. 2006, pp. 1–6.

[27] S. Atapattu, C. Tellambura, and H. Jiang, *Energy Detection for Spectrum Sensing in Cognitive Radio*. New York, NY, USA: Springer, 2014. Accessed: Apr. 10, 2021, doi: 10.1007/978-1-4939-0494-5.

[28] M. R. Manesh, M. S. Apu, N. Kaabouch, and W.-C. Hu, "Performance evaluation of spectrum sensing techniques for cognitive radio systems," in *Proc. IEEE 7th Annu. Ubiquitous Comput., Electron. Mobile Commun. Conf. (UEMCON)*, Oct. 2016, pp. 1–6.

[29] S. Nandakumar, T. Velmurugan, U. Thiagarajan, M. Karuppiah, M. M. Hassan, A. Alelaiwi, and M. M. Islam, "Efficient spectrum management techniques for cognitive radio networks for proximity service," *IEEE Access*, vol. 7, pp. 43795–43805, 2019.

[30] N. Muchandi and R. Khanai, "Cognitive radio spectrum sensing: A survey," in *Proc. Int. Conf. Electr., Electron., Optim. Techn. (ICEEOT)*, Mar. 2016, pp. 3233–3237.

[31] P. Avinash, R. Gandhiraj, and P. Soman, "Spectrum sensing using compressed sensing techniques for sparse multiband signals," *Int. J. Sci. Eng. Res.*, vol. 3, no. 5, pp. 1–5, May 2012.

[32] R. B. Patil, K. D. Kulat, and A. S. Gandhi, "SDR based energy detection spectrum sensing in cognitive radio for real time video transmission," *Model. Simul. Eng.*, vol. 2018, pp. 1–10, Apr. 2018.
[33] S. Taruna and B. Pahwa, "A novel scheme to improve the spectrum sensing performance," *Int. J. Comput. Netw. Commun.*, vol. 6, no. 3, pp. 51–58, May 2014.

ANTÓNIO BRITO (Student Member, IEEE) received the Licenciado and M.Sc. degrees in informatics and telecommunications engineering from the Instituto Superior de Ciências do Trabalho e da Empresa, University of Lisbon, in 2017 and 2018, respectively. He is currently pursuing the Ph.D. degree in information science and technology. Recently, he participated in the CONQUEST (CMU/ECE/0030/2017), an Exploratory Project from Carnegie Mellon University (CMU), Portugal, a collaboration with the Department of Engineering and Public Policy. His current research interests include cognitive radio, spectrum sensing and sharing, drone small cells, and 5G communications.

PEDRO SEBASTIÃO (Member, IEEE) received the Ph.D. degree in electrical and computer engineering from IST.

He is currently a Professor with the Information Science and Technology Department, ISCTE-Instituto Universitário de Lisboa. He is also the Board Director of the AUDAX ISCTE-Innovation and Entrepreneurship Centre, ISCTE, responsible for Public National and International Projects and Innovation & Entrepreneurship Programs, and also he is also a Researcher with the Institute of Telecommunications. His research interests include monitoring, control and communications of drones, unmanned vehicles, planning tools, stochastic process (modeling and efficient simulations), the Internet of Things, efficient communication systems, and business models. He has oriented several M.Sc. and Ph.D. thesis. He is the author or coauthor of more than 200 scientific articles and he has been responsible for several national and international research and development projects. He has been an Expert and an Evaluator of more than 100 national and international Civil and Defense Research and Development and Innovation Projects. It has several scientific, engineering and pedagogical awards. Also, he has organized or co-organized more than 50 national and international scientific conferences. He planned and developed several postgraduate courses in technologies and management, entrepreneurship and innovation and transfer of technology and innovation. He has supported several national and international projects involving technology transfer and creation of start-ups and spinoffs of value to society and market. He developed his professional activity in the National Defence Industries, initially in the Office of Studies and later as the Board Director of the Quality Department of the Production of New Products and Technologies. He was also responsible by several technologies of communications systems at Nokia-Siemens (Business Unity).

FERNANDO J. VELEZ (Senior Member, IEEE) received the Licenciado, M.Sc., and Ph.D. degrees in electrical and computer engineering from the Instituto Superior Técnico, Technical University of Lisbon, in 1993, 1996, and 2001, respectively. Since 1995, he has been with the Department of Electromechanical Engineering, Universidade da Beira Interior, Covilhã, Portugal, where he is currently an Assistant Professor. He is also a Senior Researcher with the Instituto de Telecomunicações. He was an IEF Marie Curie Research Fellow with the King's College London (KCL), in September 2008 (OPTIMOBILE IEF), and a Marie Curie ERG Fellow with the Universidade da Beira Interior, from 2010 to 2013 (PLANOPTI ERG). He is the Coordinator of the Instituto de Telecomunicações Team in the Marie Skłodowska-Curie ITN Action (TeamUp5G) that started, in 2019. He made or makes part of the teams of several European and Portuguese research projects on mobile communications, and he was the Coordinator of six Portuguese Projects. Recently, he was the Coordinator of CONQUEST (CMU/ECE/0030/2017), an Exploratory Project with Carnegie Mellon University (CMU), Portugal, a collaboration with the Department of Engineering and Public Policy from CMU. He has authored three books, 24 book chapters, 160 papers and communications in international journals and conferences, plus 39 in national conferences. He is currently the IEEE VTS Region 8 (Europe, Middle East, and Africa) Chapter Coordinator (nominated by VTS in 2010) and was the elected as the IEEE VTS Portugal Chapter coordinator, from 2006 to 2014. He is also an Adjunct Coordinator of the Telecommunications Specialization of Ordem dos Engenheiros. He was the Coordinator of the WG2 (on cognitive radio/software defined radio coexistence studies) of COST IC0905 TERRA. His research interests include cellular planning tools, traffic from mobility, wireless body sensor networks and wearable technologies, cross-layer design, spectrum sharing/aggregation, and cost/revenue performance of advanced mobile communication systems.